Supplementary Table S1. Patient and Clinical Phenotype Characteristics of the Study Cohorts.

	level	Overall	LIFE-Adult	LIFE-Heart-Cases	LIFE-Heart-Controls	PROGRESS
n		1306	400	126	400	380
AGE (mean (SD))		61.06 (12.50)	61.96 (9.22)	64.49 (9.95)	61.97 (9.17)	58.00 (17.68)
Plaque Score (mean (SD))		1.06 (1.27)	0.26 (0.53)	1.93 (1.32)	1.85 (1.29)	NaN (NA)
SOFA Score (mean (SD))		3.64 (3.00)	NaN (NA)	NaN (NA)	NaN (NA)	3.64 (3.00)
Inclusion (%)	TRUE	1306 (100.0)	400 (100.0)	126 (100.0)	400 (100.0)	380 (100.0)
Day of Enrollment (%)	0	363 (27.8)	0 (0.0)	0 (0.0)	0 (0.0)	363 (95.5)
	1	13 (1.0)	0 (0.0)	0 (0.0)	0 (0.0)	13 (3.4)
	2	3 (0.2)	0 (0.0)	0 (0.0)	0 (0.0)	3 (0.8)
	3	1 (0.1)	0 (0.0)	0 (0.0)	0 (0.0)	1 (0.3)
		926 (70.9)	400 (100.0)	126 (100.0)	400 (100.0)	0 (0.0)
STROKE (%)	FALSE	795 (60.9)	399 (99.8)	4 (3.2)	392 (98.0)	0 (0.0)
	TRUE	28 (2.1)	0 (0.0)	28 (22.2)	0 (0.0)	0 (0.0)
	NA	483 (37)	1 (0.2)	94 (74.6)	8 (2.0)	380 (100.0)
Myocardial Infarction (%)	FALSE	823 (63.0)	400 (100.0)	1 (0.8)	381 (95.2)	41 (10.8)
	TRUE	76 (5.8)	0 (0.0)	76 (60.3)	0 (0.0)	0 (0.0)
	NA	407 (31.2)	0 (0.0)	49 (38.9)	19 (4.8)	339 (89.2)
Cardiovascular Death (%)	FALSE	493 (37.7)	0 (0.0)	93 (73.8)	400 (100.0)	0 (0.0)
	TRUE	33 (2.5)	0 (0.0)	33 (26.2)	0 (0.0)	0 (0.0)
	NA	780 (59.7)	400 (100.0)	0 (0.0)	0 (0.0)	380 (100.0)
Follow up with cardiovascular endpoint (%)	FALSE	907 (69.4)	381 (95.2)	126 (100.0)	400 (100.0)	0 (0.0)
	TRUE	19 (1.5)	19 (4.8)	0 (0.0)	0 (0.0)	0 (0.0)
	NA	380 (29.1)	0 (0.0)	0 (0.0)	0 (0.0)	380 (100.0)
SEX (%)	FEMALE	337 (25.8)	81 (20.2)	24 (19.0)	81 (20.2)	151 (39.7)
	MALE	969 (74.2)	319 (79.8)	102 (81.0)	319 (79.8)	229 (60.3)
LMCAD (%)	FALSE	369 (28.3)	0 (0.0)	90 (71.4)	279 (69.8)	0 (0.0)
	TRUE	157 (12.0)	0 (0.0)	36 (28.6)	121 (30.2)	0 (0.0)
	NA	780 (59.7)	400 (100.0)	0 (0.0)	0 (0.0)	380 (100.0)
CAD (%)	TRUE	526 (40.3)	0 (0.0)	126 (100.0)	400 (100.0)	0 (0.0)
	NA	780 (59.7)	400 (100.0)	0 (0.0)	0 (0.0)	380 (100.0)
CAD without prior MI (%)	FALSE	39 (3.0)	0 (0.0)	0 (0.0)	0 (0.0)	39 (10.3)
	NA	1267 (97.0)	400 (100.0)	126 (100.0)	400 (100.0)	341 (89.7)
Heart Failure (%)	FALSE	366 (28.0)	0 (0.0)	0 (0.0)	0 (0.0)	366 (96.3)
	NA	940 (72.0)	400 (100.0)	126 (100.0)	400 (100.0)	14 (3.7)

This table provides a summary of the baseline characteristics and clinical phenotypes for the three study cohorts: PROGRESS, LIFE-Adult, and LIFE-Heart. Data are presented as mean (standard deviation) for continuous variables and as number (percentage) for categorical variables.

Abbreviations: SOFA, Sequential Organ Failure Assessment; CAP, community-acquired pneumonia; CAD, coronary artery disease; NA, not applicable; LMCAD, Left Main Coronary Artery Stenosis; MI, Myocardial Infarction.

Supplementary Table S2. LC-MS/MS parameter for sphingolipid quantification.

Sphingolipid	**Precursor ion (*m/z*)**	**Product ion (*m/z*)** [a]	**ISTD**	**Calibration reference compound**
d_7-Sph (ISTD)	307.3 $[M+H]^+$	289.3 / **259.3**	-	-
d_7-S1P (ISTD)	387.3 $[M+H]^+$	**271.3** / 82.1	-	-
Sph	300.3 $[M+H]^+$	282.3 / **252.3**	d_7-Sph	-
S1P	380.3 $[M+H]^+$	**264.3** / 82.1	d_7-S1P	-
dhS1P	382.3 $[M+H]^+$	**284.3** / 266.4	d_7-S1P	-
dhCer 16:0	540.5 $[M+H]^+$	522.6 / **284.3**	Cer 17:0	dhCer 16:0
dhCer 18:0	568.5 $[M+H]^+$	550.5 / **284.3**	Cer 17:0	dhCer 18:0
dhCer 20:0	596.6 $[M+H]^+$	578.6 / **284.3**	Cer 17:0	dhCer 18:0
dhCer 22:0	624.6 $[M+H]^+$	606.6 / **284.3**	Cer 17:0	dhCer 24:0
dhCer 24:0	652.7 $[M+H]^+$	634.6 / **284.3**	Cer 17:0	dhCer 24:0
dhCer 24:1	650.7 $[M+H]^+$	632.7 / **284.3**	Cer 17:0	dhCer 24:1
Cer 17:0 (ISTD)	534.5 $[M-H_2O+H]^+$	282.3 / **264.3**	-	-
Cer 16:0	520.5 $[M-H_2O+H]^+$	282.3 / **264.3**	Cer 17:0	Cer 16:0
Cer 18:0	548.5 $[M-H_2O+H]^+$	282.3 / **264.2**	Cer 17:0	Cer 18:0
Cer 20:0	576.6 $[M-H_2O+H]^+$	282.3 / **264.3**	Cer 17:0	Cer 20:0
Cer 22:0	604.6 $[M-H_2O+H]^+$	282.3 / **264.3**	Cer 17:0	Cer 22:0
Cer 24:0	632.6 $[M-H_2O+H]^+$	282.3 / **264.3**	Cer 17:0	Cer 24:0
Cer 24:1	630.6 $[M-H_2O+H]^+$	282.3 / **264.3**	Cer 17:0	Cer 24:1
dhSM 16:0	705.6 $[M+H]^+$	**184.0** / 86.1	d_{31}-SM 16:0	SM 16:0
dhSM 18:0	733.6 $[M+H]^+$	**184.0** / 86.1	d_{31}-SM 16:0	SM 18:0
dhSM 20:0	761.6 $[M+H]^+$	**184.0** / 86.1	d_{31}-SM 16:0	SM 20:0
dhSM 22:0	789.7 $[M+H]^+$	**184.0** / 86.1	d_{31}-SM 16:0	SM 22:0
dhSM 24:0	817.7 $[M+H]^+$	**184.0** / 86.1	d_{31}-SM 16:0	SM 24:0
dhSM 24:1	815.7 $[M+H]^+$	184.0 / **86.1**	d_{31}-SM 16:0	SM 24:1
d_{31}-SM 16:0 (ISTD)	734.6 $[M+H]^+$	**184.0** / 86.1	-	-
SM 14:0	675.5 $[M+H]^+$	**184.0** / 86.1	d_{31}-SM 16:0	SM 18:0
SM 16:0	703.6 $[M+H]^+$	**184.0** / 86.1	d_{31}-SM 16:0	SM 16:0
SM 18:0	731.6 $[M+H]^+$	**184.0** / 86.1	d_{31}-SM 16:0	SM 18:0
SM 20:0	759.6 $[M+H]^+$	**184.0** / 86.1	d_{31}-SM 16:0	SM 20:0
SM 22:0	787.7 $[M+H]^+$	**184.0** / 86.1	d_{31}-SM 16:0	SM 22:0
SM 24:0	815.7 $[M+H]^+$	**184.0** / 86.1	d_{31}-SM 16:0	SM 24:0
SM 24:1	813.7 $[M+H]^+$	184.0 / **86.1**	d_{31}-SM 16:0	SM 24:1
HexCer 17:0 (ISTD)	714.6 $[M+H]^+$	696.6 / **264.2**	-	-
HexCer 16:0	700.6 $[M+H]^+$	682.6 / **264.2**	HexCer 17:0	HexCer 16:0
HexCer 18:0	728.6 $[M+H]^+$	710.6 / **264.2**	HexCer 17:0	HexCer 16:0
HexCer 20:0	756.6 $[M+H]^+$	738.6 / **264.2**	HexCer 17:0	HexCer 16:0
HexCer 22:0	784.6 $[M+H]^+$	766.6 / **264.2**	HexCer 17:0	HexCer 24:1
HexCer 24:0	812.7 $[M+H]^+$	794.7 / **264.2**	HexCer 17:0	HexCer 24:1
HexCer 24:1	810.7 $[M+H]^+$	792.7 / **264.2**	HexCer 17:0	HexCer 24:1
LacCer 17:0 (ISTD)	876.6 $[M+H]^+$	534.5 / **264.3**	-	-
LacCer 16:0	862.6 $[M+H]^+$	520.5 / **264.3**	LacCer 17:0	LacCer 16:0
LacCer 18:0	890.6 $[M+H]^+$	548.5 / **264.3**	LacCer 17:0	LacCer 16:0
LacCer 20:0	918.6 $[M+H]^+$	576.6 / **264.3**	LacCer 17:0	LacCer 16:0
LacCer 22:0	946.6 $[M+H]^+$	604.6 / **264.3**	LacCer 17:0	LacCer 24:1
LacCer 24:0	974.7 $[M+H]^+$	632.6 / **264.3**	LacCer 17:0	LacCer 24:1
LacCer 24:1	972.7 $[M+H]^+$	630.7 / **264.3**	LacCer 17:0	LacCer 24:1

Precursor ion *(m/z)* represents the mass-to-charge ratio of the intact ion selected in the first quadrupole (Q1). Product ion *(m/z)* denotes the fragment ions generated via collision-induced dissociation and selected in the third quadrupole (Q3); bold values indicate the quantifier ion used for calculation. Calibration reference compound refers to the specific standard used to construct the calibration curve for quantification.

Abbreviations: Cer, ceramide; dhCer, dihydroceramide; dhS1P, dihydrosphingosine 1-phosphate, dhSM, dihydrosphingomyelin; HexCer, hexosylceramide; ISTD, internal standard; LacCer, lactosylceramide; S1P, sphingosine 1-phosphate; SM, sphingomyelin; Sph, sphingosine.

Supplementary Figure S1. Data quality control and preprocessing.

(A) Principal component analysis (PCA) of the raw metabolomics data, with samples colored by analytical batch. The distinct clustering of batches (e.g., B1-B7) indicates a strong batch effect. Notably, the PROGRESS samples, analyzed in batch 5 (B5P), form a separate cluster. (B) PCA of the data after batch correction using the EigenMS algorithm. The successful removal of batch-associated variation is demonstrated by the intermingling of samples from all batches. The B5P samples are now integrated with the other patient samples according to their biological group rather than their analytical batch. (C) PCA of the raw data colored by primary analysis group. While some underlying biological structure is visible, it is partially obscured by technical variation. (D) PCA of the final, fully preprocessed data set. After batch correction and normalization, the primary biological groups (e.g., PROGRESS vs. other groups) show clear separation, indicating that the data is ready for downstream statistical analysis.

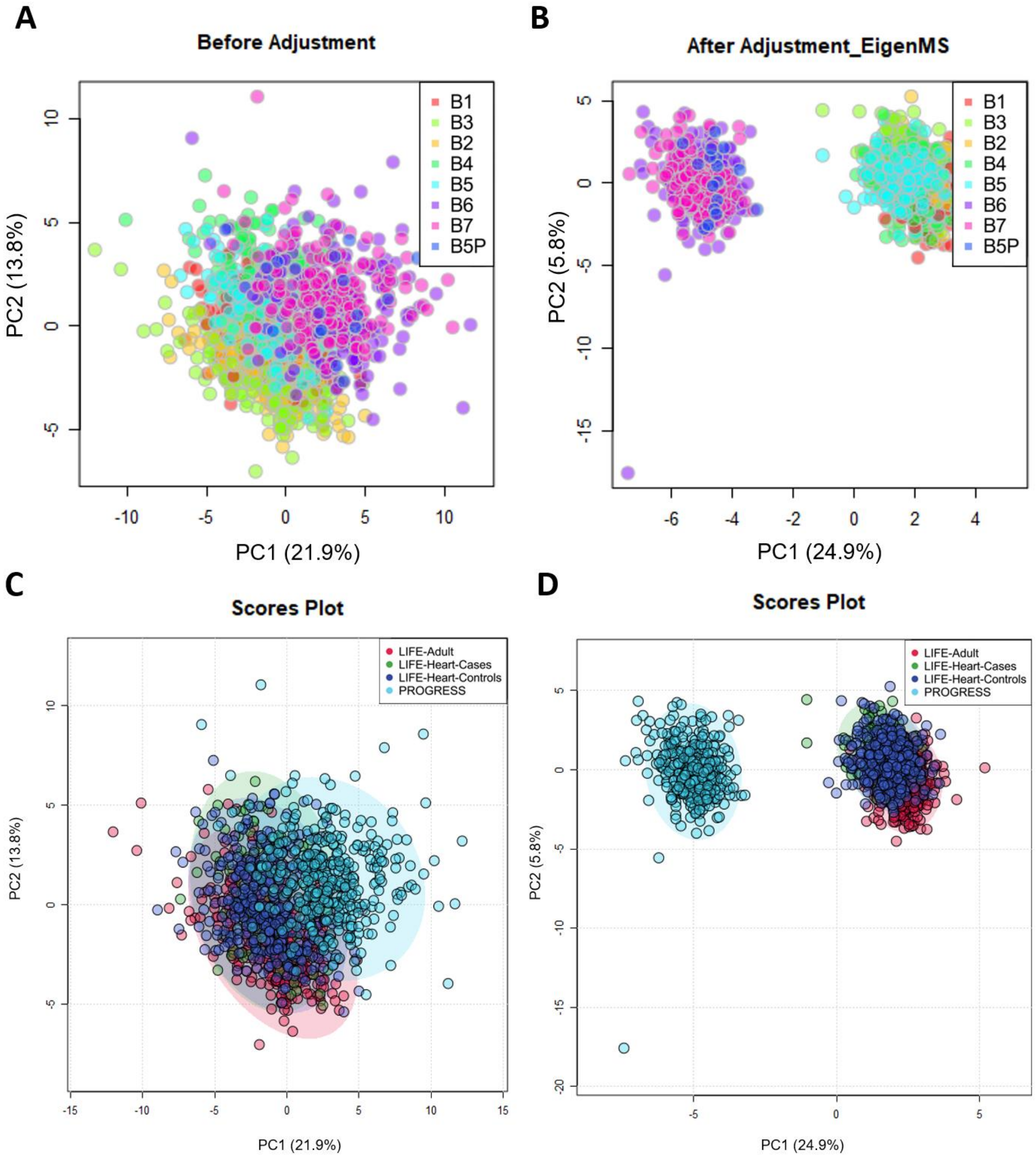

Supplementary Table S3. Differential abundance of all 43 metabolites between the PROGRESS and LIFE-Adult groups.

Metabolite	Log$_2$ Fold Change (log$_2$FC)	Q-value
dhCer 24:0	-2.01	1.00×10^{-179}
dhS1P	1.99	5.30×10^{-156}
S1P	1.94	9.50×10^{-172}
Cer 18:0	1.86	3.60×10^{-162}
Cer 16:0	1.86	4.60×10^{-159}
Cer 24:0	-1.84	3.70×10^{-132}
dhCer (total)	-1.83	7.10×10^{-164}
Cer 20:0	1.76	5.60×10^{-137}
SM 18:0	1.62	8.62×10^{-97}
dhCer 22:0	-1.61	2.00×10^{-117}
HexCer 22:0	-1.49	3.47×10^{-75}
LacCer 18:0	1.36	1.31×10^{-62}
LacCer (total)	1.34	2.74×10^{-76}
SM 14:0	-1.30	3.48×10^{-54}
dhSM 22:0	-1.28	6.91×10^{-74}
dhSM 20:0	-1.24	8.19×10^{-74}
dhCer 24:1	-1.23	7.09×10^{-68}
SM 24:0	-1.10	9.61×10^{-43}
SM 20:0	-1.09	3.81×10^{-42}
dhCer 18:0	1.06	1.16×10^{-35}
LacCer 16:0	0.96	2.19×10^{-39}
Sph	0.95	8.41×10^{-26}
HexCer 18:0	0.85	9.15×10^{-29}
Cer 24:1	0.81	1.60×10^{-23}
HexCer 16:0	0.76	2.06×10^{-20}
dhSM 18:0	0.75	5.31×10^{-20}
dhSM 24:0	-0.71	2.02×10^{-17}
dhSM (total)	-0.70	1.53×10^{-21}
HexCer 24:0	-0.67	2.74×10^{-18}
dhSM 24:1	-0.66	1.95×10^{-17}
dhSM 16:0	-0.65	2.42×10^{-17}
HexCer 20:0	-0.52	5.36×10^{-10}
dhCer 16:0	0.51	6.28×10^{-10}
LacCer 24:1	0.49	8.15×10^{-10}
LacCer 20:0	0.41	1.53×10^{-6}
HexCer (total)	-0.35	1.20×10^{-5}
LacCer 22:0	-0.28	3.21×10^{-4}
dhCer 20:0	-0.25	8.25×10^{-3}
HexCer 24:1	0.24	5.77×10^{-3}
SM 22:0	-0.21	1.34×10^{-2}
Cer 22:0	0.14	9.65×10^{-2}
LacCer 24:0	-0.01	8.78×10^{-1}
Cer (total)	0.00	9.65×10^{-1}

Metabolites (individual or subclass total) with $|\log_2 FC| > 0.5$ and q-value < 0.05 were considered significant. Results are ordered by the strength of association (highest to lowest absolute fold change). A positive log$_2$ fold change denotes increased abundance in the PROGRESS group relative to the LIFE-Adult group. Abbreviations: Cer, Ceramide; dhCer, Dihydroceramide; dhS1P, Dihydrosphingosine 1-phosphate; dhSM, Dihydrosphingomyelin, HexCer, Hexosylceramide; LacCer, Lactosylceramide; S1P, Sphingosine-1-phosphate; SM, Sphingomyelin; Sph, Sphingosine.

Supplementary Figure S2. Pathway Enrichment Analysis of 33-Pneumonia Associated Metabolites

This figure displays the results of the pathway over-representation analysis performed on the 33 metabolites found to be significantly different in pneumonia patients, showing the top 25 most enriched metabolite sets. The y-axis lists the names of the enriched biological pathways, while the x-axis represents the statistical significance of the enrichment, plotted as the -log10 of the p-value, where a higher value indicates greater significance. The visual characteristics of each point provide further detail: its size is proportional to the Enrichment Ratio, with larger points indicating a higher ratio of observed to expected metabolites within that pathway, and its color corresponds to the p-value, with deep red indicating the highest significance. As expected, given that all 33 input metabolites are sphingolipids, the analysis confirmed that pathways related to sphingolipid metabolism were the most prominently and significantly enriched. Several lysosomal storage disorders associated with sphingolipid breakdown, such as Fabry, Gaucher, and Krabbe disease, are also among the top hits.

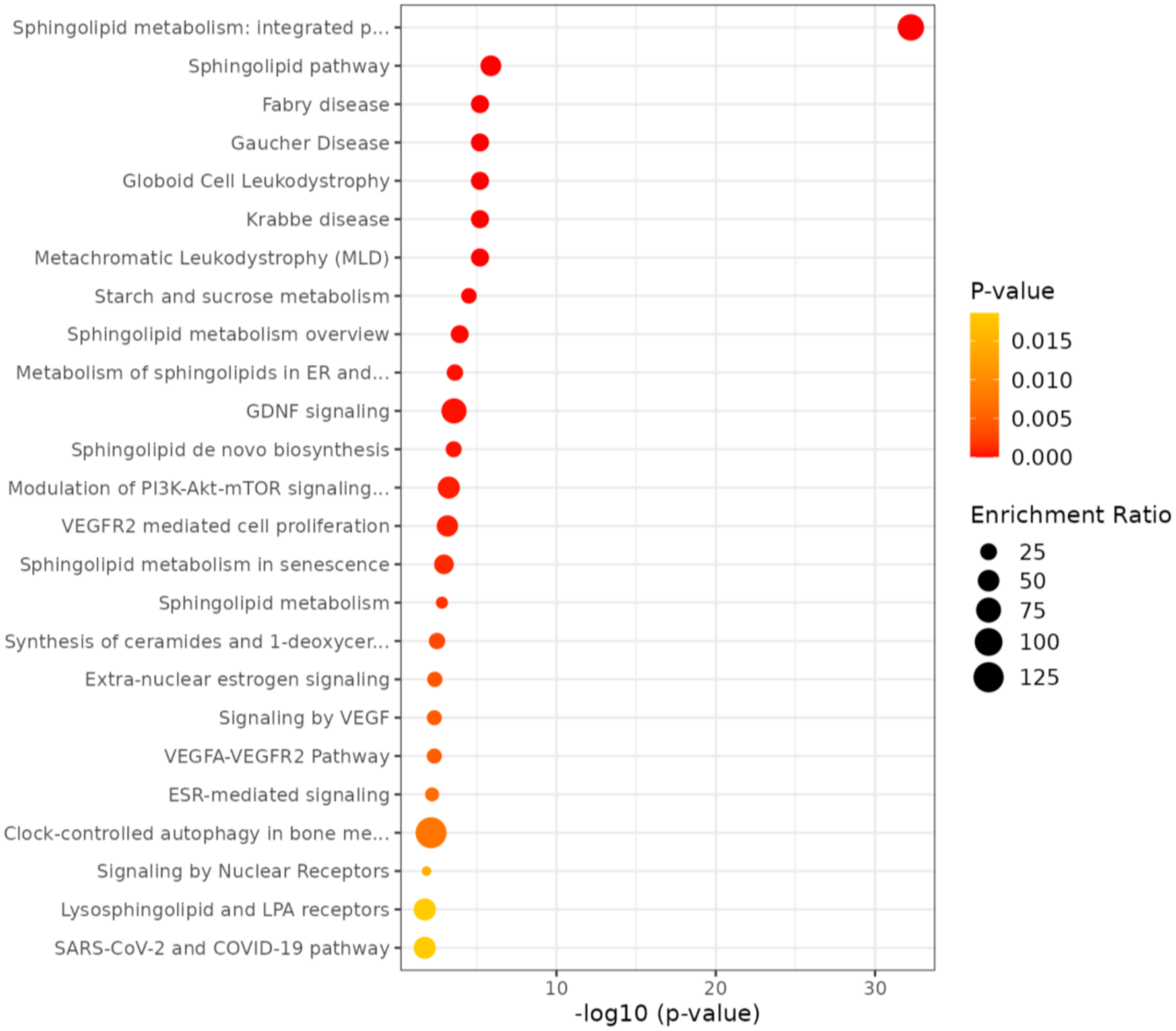

Supplementary Figure S3. Concordance of 33 Pneumonia Associated Metabolites with Disease Severity

Heatmap displaying the relationship between pneumonia status and disease severity for 33 pneumonia-associated metabolites. The left column shows the log2fold change (log2FC) in pneumonia vs. controls, while the right column shows the association coefficient with the SOFA score at baseline. To allow direct comparison between these distinct metrics, values were column-scaled (Z-score): red indicates upregulation in pneumonia or a positive association with higher SOFA scores, while blue indicates downregulation or a negative association. Rows are organized by hierarchical clustering using a sign-symmetric distance measure (1−|*r*|), where *r* is the partial Pearson correlation coefficient adjusted for age, sex, diabetes status, eGFR, and study group. Asterisks (*) denote statistical significance, defined as: $q < 0.05$ & $|\log_2 FC| > 0.5$ for the Pneumonia contrast; and $q<0.25$ for the association with SOFA score. The red annotation bar ('Concordance') highlights metabolites showing a significant and directionally concordant effect in both analyses.

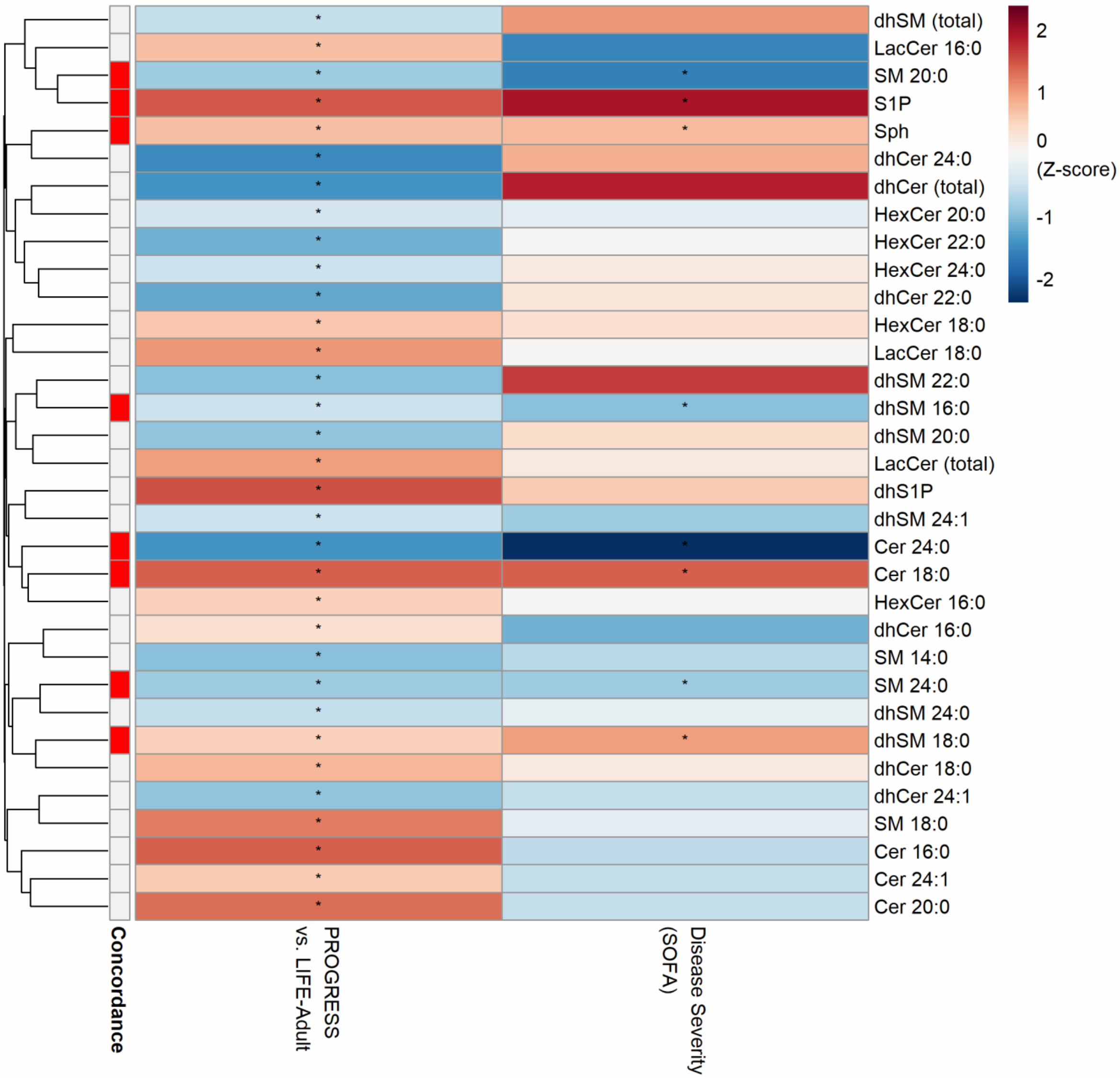

Supplementary Table S4. Association of Pneumonia-Associated Metabolites with Disease Severity.

Metabolite	Estimate (β)	Q-value
Cer 24:0	-0.65	0.004
SM 20:0	-0.43	0.008
S1P	0.60	0.010
LacCer 16:0	-0.42	0.035
dhSM 22:0	0.51	0.043
dhCer 16:0	-0.29	0.058
Cer 18:0	0.44	0.106
dhCer (total)	0.56	0.106
dhSM (total)	0.33	0.106
dhSM 18:0	0.32	0.111
Sph	0.25	0.158
dhSM 16:0	-0.24	0.243
SM 24:0	-0.21	0.248
dhS1P	0.21	0.395
dhSM 24:1	-0.21	0.395
SM 14:0	-0.15	0.431
HexCer 18:0	0.14	0.520
dhCer 24:0	0.28	0.578
dhCer 18:0	0.10	0.597
Cer 24:1	-0.12	0.597
dhSM 20:0	0.15	0.597
Cer 20:0	-0.13	0.638
Cer 16:0	-0.13	0.638
LacCer (total)	0.10	0.650
dhCer 24:1	-0.12	0.677
HexCer 24:0	0.10	0.677
dhCer 22:0	0.11	0.790
HexCer 16:0	0.04	0.847
LacCer 18:0	0.04	0.864
HexCer 22:0	0.04	0.889
SM 18:0	-0.03	0.896
HexCer 20:0	-0.02	0.906
dhSM 24:0	-0.01	0.919

The table presents association results for the 33 pneumonia associated metabolites with disease severity operationalized by the SOFA score. Results were derived from multivariable linear regression models, adjusted for age, sex, eGFR, and diabetes status. A positive β-estimate indicates that higher metabolite levels are associated with a higher SOFA score. The table is ordered by the absolute β-estimate in descending order. Significance was determined using a Benjamini-Hochberg false discovery rate (FDR) threshold of $q < 0.25$.

Abbreviations: Cer, Ceramide; dhCer, Dihydroceramide; dhS1P, Dihydrosphingosine 1-phosphate; dhSM, Dihydrosphingomyelin, HexCer, Hexosylceramide; LacCer, Lactosylceramide; S1P, Sphingosine 1-phosphate; SM, Sphingomyelin; Sph, Sphingosine.

Supplementary Figure S4. Volcano plot for the differential abundance of the 33-metabolite pneumonia signature between stable CAD and healthy controls.

Each point represents one of the 33 metabolites from the pneumonia associated signature. The x-axis shows the $\log_2$ fold change, and the y-axis shows the $-\log_{10}$ of the Benjamini-Hochberg adjusted p-value (q-value). Metabolites meeting the significance threshold ($q < 0.05$) are highlighted, with red indicating upregulation and blue indicating downregulation in the LIFE-Heart controls group (stable CAD). The horizontal dashed line represents the significance threshold. The top 10 most significant metabolites are labeled.

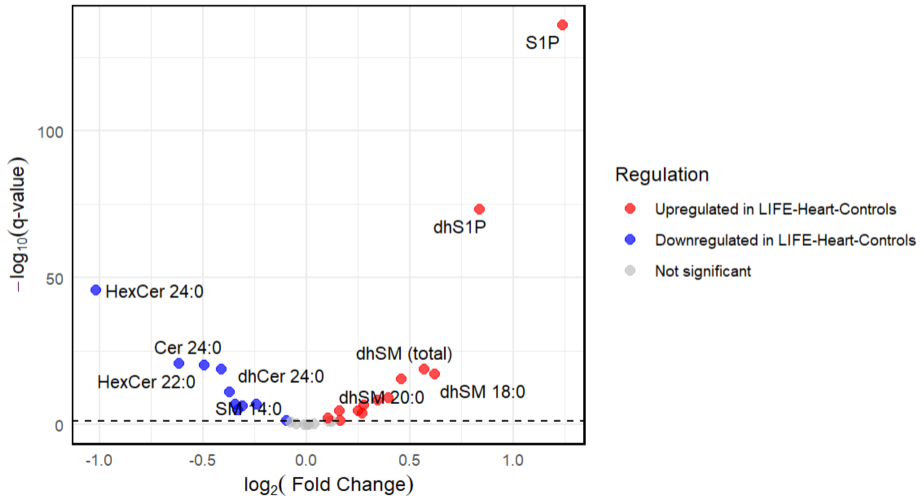

Supplementary Table S5. Differential abundance of the 33-metabolite pneumonia signature between the LIFE-Heart-Controls and LIFE-Adult groups.

Metabolite	Log$_2$ Fold Change (log$_2$FC)	Q-value
S1P	1.24	6.10×10^{-137}
HexCer 24:0	-1.02	1.12×10^{-46}
dhS1P	0.84	4.61×10^{-74}
dhSM 18:0	0.62	5.52×10^{-18}
HexCer 22:0	-0.62	1.26×10^{-21}
dhSM (total)	0.57	9.28×10^{-20}
Cer 24:0	-0.49	3.66×10^{-21}
dhSM 20:0	0.46	2.68×10^{-16}
dhCer 24:0	-0.41	1.07×10^{-19}
dhCer 16:0	0.39	6.61×10^{-10}
SM 14:0	-0.37	5.32×10^{-12}
Cer 24:1	-0.35	1.07×10^{-7}
dhCer 18:0	0.34	5.20×10^{-9}
HexCer 20:0	-0.33	8.54×10^{-6}
LacCer 16:0	-0.31	2.68×10^{-7}
SM 18:0	0.28	1.94×10^{-7}
dhSM 24:1	0.27	8.21×10^{-5}
dhSM 22:0	0.25	1.19×10^{-5}
LacCer (total)	-0.24	1.16×10^{-7}
dhSM 24:0	0.16	2.72×10^{-2}
Cer 18:0	0.16	2.06×10^{-5}
Sph	0.12	8.48×10^{-2}
dhCer 24:1	0.10	9.02×10^{-2}
Cer 16:0	0.10	4.37×10^{-3}
dhCer (total)	-0.10	3.96×10^{-2}
dhCer 22:0	-0.08	1.72×10^{-1}
HexCer 18:0	-0.05	4.65×10^{-1}
SM 20:0	0.04	6.08×10^{-1}
dhSM 16:0	-0.01	9.42×10^{-1}
LacCer 18:0	0.01	9.42×10^{-1}
HexCer 16:0	0.01	9.42×10^{-1}
SM 24:0	0.00	9.42×10^{-1}
Cer 20:0	0.00	9.42×10^{-1}

We analyzed the 33 pneumonia associated metabolites for association with stable CAD case/control status. Significance in this analysis was defined as q-value < 0.05. The results are ordered by decreasing absolute fold change. A positive log$_2$ fold change denotes increased abundance in the stable CAD group (LIFE-Heart controls).

Abbreviations: Cer, Ceramide; dhCer, Dihydroceramide; dhS1P, Dihydrosphingosine 1-phosphate; dhSM, Dihydrosphingomyelin, HexCer, Hexosylceramide; LacCer, Lactosylceramide; S1P, Sphingosine 1-phosphate; SM, Sphingomyelin; Sph, Sphingosine.

Supplementary Figure S5. Volcano plot for the differential abundance of pneumonia associated metabolites between stable and unstable CAD.

Each point represents one of the 33 metabolites associated with pneumonia case/control status. The x-axis shows the $\log_2$ fold change, and the y-axis shows the $-\log_{10}$ of the Benjamini-Hochberg adjusted p-value (q-value). Metabolites meeting the significance threshold ($q < 0.05$) are highlighted, with red indicating upregulation and blue indicating downregulation in the unstable CAD group (LIFE-Heart cases). The horizontal dashed line represents the significance threshold. The top 10 most significant metabolites are labeled.

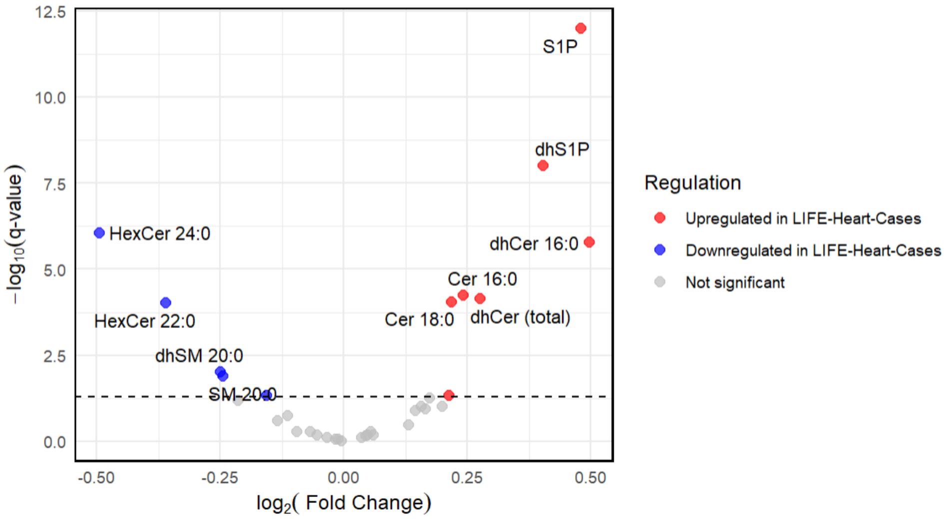

Supplementary Table S6. Differential abundance of pneumonia associated metabolites between stable and unstable CAD.

Metabolite	Log_2 Fold Change (log_2FC)	Q-value
dhCer 16:0	0.50	1.61×10^{-6}
HexCer 24:0	-0.49	8.53×10^{-7}
S1P	0.48	9.95×10^{-13}
dhS1P	0.40	9.58×10^{-9}
HexCer 22:0	-0.36	9.36×10^{-5}
dhCer (total)	0.28	7.04×10^{-5}
dhSM 20:0	-0.25	9.22×10^{-3}
SM 20:0	-0.25	1.27×10^{-2}
Cer 16:0	0.24	5.57×10^{-5}
Cer 18:0	0.22	8.55×10^{-5}
dhSM 24:1	-0.21	6.46×10^{-2}
dhCer 24:1	0.21	4.57×10^{-2}
dhSM 18:0	0.20	9.59×10^{-2}
SM 18:0	0.17	5.33×10^{-2}
dhCer 18:0	0.16	1.10×10^{-1}
LacCer (total)	-0.16	4.57×10^{-2}
SM 24:0	0.16	9.59×10^{-2}
dhCer 22:0	0.14	1.23×10^{-1}
HexCer 16:0	-0.13	2.51×10^{-1}
dhSM 16:0	0.13	3.29×10^{-1}
LacCer 18:0	-0.11	1.79×10^{-1}
HexCer 20:0	-0.10	4.97×10^{-1}
Cer 24:0	-0.07	4.97×10^{-1}
Cer 24:1	0.06	6.43×10^{-1}
dhCer 24:0	0.05	4.97×10^{-1}
LacCer 16:0	-0.05	6.43×10^{-1}
Sph	0.05	6.43×10^{-1}
SM 14:0	0.04	6.83×10^{-1}
HexCer 18:0	0.04	7.52×10^{-1}
dhSM 22:0	-0.03	7.52×10^{-1}
dhSM (total)	-0.02	8.66×10^{-1}
Cer 20:0	-0.01	8.66×10^{-1}
dhSM 24:0	-0.01	9.55×10^{-1}

We compared the 33 metabolites associates with pneumonia case/control status between stable and unstable CAD casese. Significance in this analysis was defined as q-value < 0.05. The results are ordered by decreasing absolute fold change. A positive log_2 fold change denotes increased abundance in unstable CAD cases (LIFE-Heart cases).

Abbreviations: Cer, Ceramide; dhCer, Dihydroceramide; dhS1P, Dihydrosphingosine 1-phosphate; dhSM, Dihydrosphingomyelin, HexCer, Hexosylceramide; LacCer, Lactosylceramide; S1P, Sphingosine 1-phosphate; SM, Sphingomyelin; Sph, Sphingosine.

Supplementary Figure S6. Confounder-Adjusted Correlation Matrix of all 43 Measured Metabolites.

This heatmap displays the Spearman correlation coefficients among all 43 metabolites included in the study. To account for potential confounding variables, correlations were calculated on the residuals from linear models adjusted for cohort (Class), age, sex, eGFR, and diabetes. Red squares indicate a positive correlation and blue squares indicate a negative correlation, with color intensity proportional to the strength of the association. Numerical values are shown only for correlations that were statistically significant ($p < 0.05$). Metabolite labels are colored to indicate their classification from the multi-stage analysis. Labels in red denote the 17 metabolites, which were significant in the pneumonia case/control analysis and also dysregulated with a concordant direction of change in at least one cardiovascular disease context.

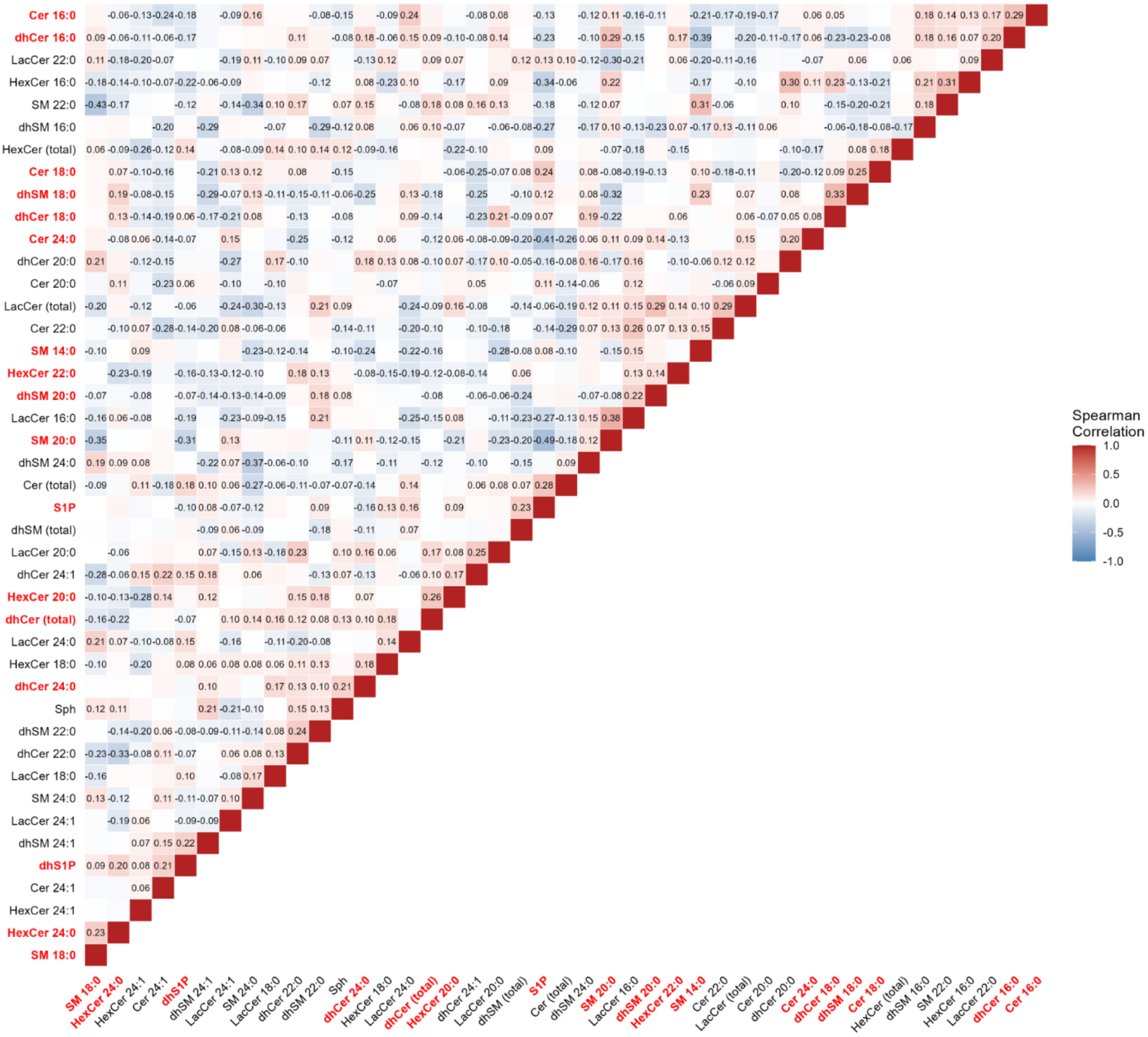

Supplementary Table S7. Overview of GWAS summary statistics used for Mendelian Randomization.

Trait	Abbreviation	GWAS Catalogue Accession
LDL Cholesterol	LDL-C	GCST90002412 [1]
Sphingosine 1-phosphate	S1P	GCST90199657 [2]
Sphinganine 1-phosphate	dhS1P	GCST90199845 [2]
C14:0 Sphingomyelin (SM(d18:1/14:0))	SM 14:0	GCST009391 [3]
C18:0 Sphingomyelin (SM(d18:1/18:0))	SM 18:0	GCST90134400 [4]
C16:0 Ceramide (Cer(d18:1/16:0))	Cer 16:0	GCST90024670 [5]
C18:0 Ceramide (Cer(d18:1/18:0))	Cer 18:0	GCST90024043 [5]
C24:0 Ceramide (Cer(d18:1/24:0))	Cer 24:0	GCST90024046 [5]
Coronary Artery Disease	CAD	GCST003116 [6]

Trait specifies the clinical phenotype or metabolite analyzed; specific lipid notations (e.g., d18:1/14:0) indicate the sphingoid base (e.g., d18:1) and fatty acyl chain (e.g., 14:0) composition. Abbreviation denotes the short identifier used throughout the manuscript. GWAS Catalogue Accession provides the unique study ID from the NHGRI-EBI GWAS Catalog, with the corresponding original publication citation provided in brackets. All summary-level genetic data were obtained from studies of European ancestry to ensure the validity of the two-sample MR design.

Supplementary Figure S7. Mendelian Randomization scatter plot for the causal effect of Ceramide 18:0 on Coronary Artery Disease (CAD).

Each point represents a single genetic instrument (SNP), plotting the SNP's effect on Cer 18:0 levels (x-axis) against its effect on CAD risk (y-axis). Error bars indicate the standard errors for each effect estimate. The colored lines show the causal estimates derived from different MR methods. The slopes of these lines, all centered around zero, indicate a null causal effect. The consistency across methods (Inverse Variance Weighted, MR-Egger, Weighted Median) demonstrates the robustness of this null finding and suggests no significant directional pleiotropy.

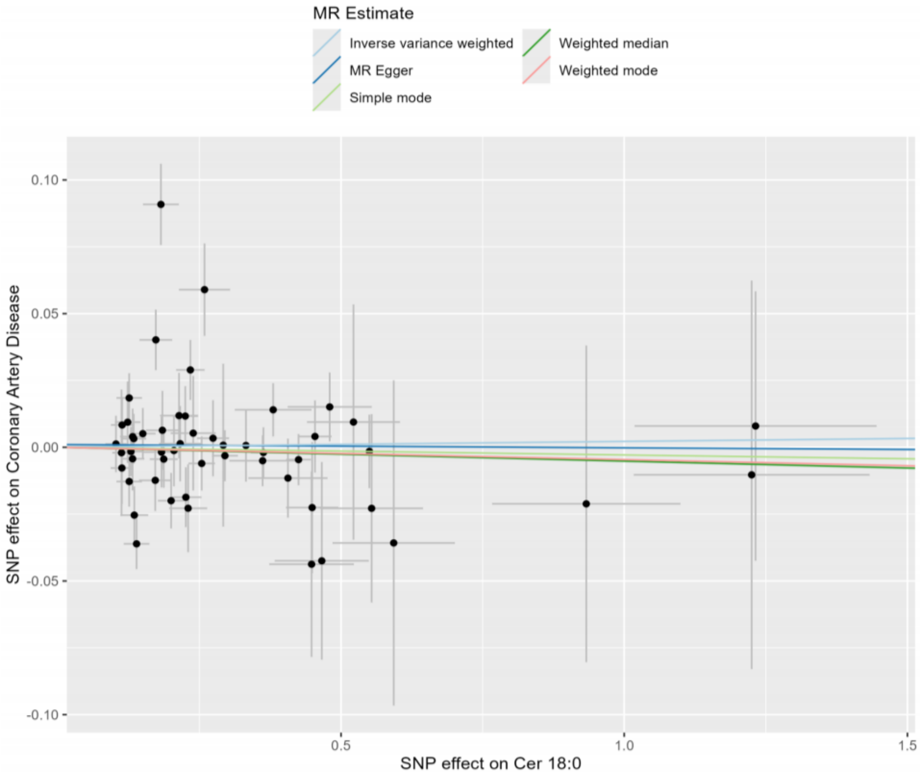

Supplementary Figure S8. Comparison of Total Cholesterol Levels Between Study Cohorts.

The figure displays the adjusted mean total cholesterol levels for each of the four study cohorts. Means were estimated from a multivariable linear model after accounting for the effects of age, sex, eGFR, diabetes and statin treatment. The points represent the estimated adjusted means, and the vertical error bars represent the respective 95% confidence intervals. The plot visually demonstrates that the total cholesterol level in the PROGRESS cohort is significantly lower than in the LIFE-Adult, LIFE-Heart-Controls, and LIFE-Heart-Cases cohorts, as indicated by the non-overlapping confidence intervals. We conclude that cholesterol is strongly down-regulated in pneumonia.

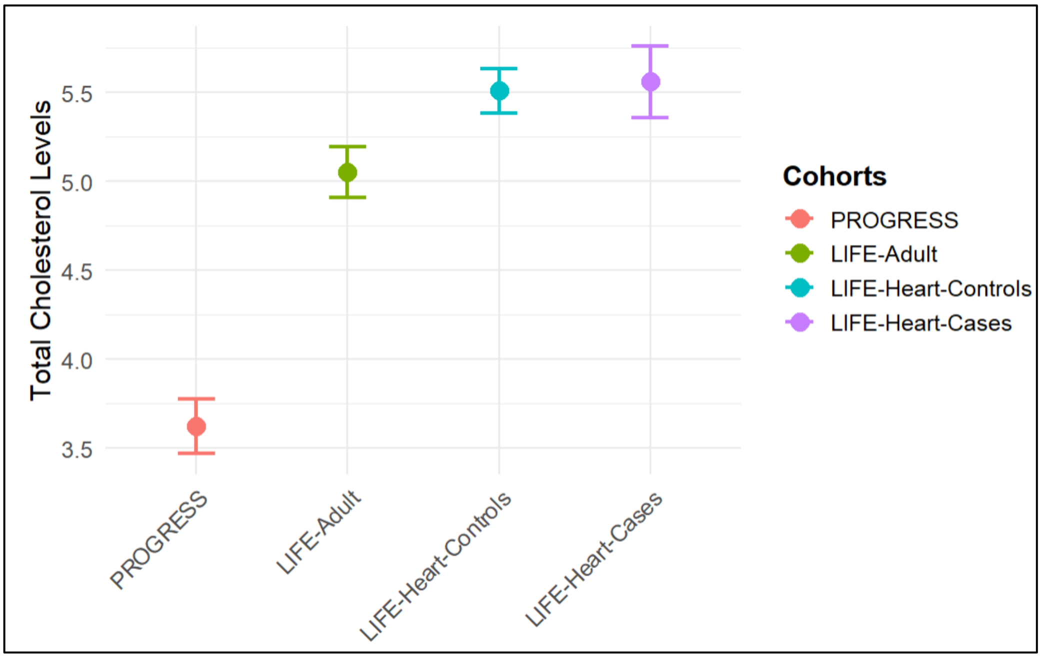

References

[1] Y. C. Klimentidis, A. Arora, M. Newell, J. Zhou, J. M. Ordovas, B. J. Renquist and A. C. Wood, "Phenotypic and Genetic Characterization of Lower LDL Cholesterol and Increased Type 2 Diabetes Risk in the UK Biobank," *Diabetes,* vol. 69, no. 10, pp. 2194-2205, 10 2020.

[2] Y. Chen, T. Lu, U. Pettersson-Kymmer, I. D. Stewart, G. Butler-Laporte, T. Nakanishi, A. Cerani, K. Y. H. Liang, S. Yoshiji, J. D. S. Willett, C.-Y. Su, P. Raina, C. M. T. Greenwood, Y. Farjoun, V. Forgetta, C. Langenberg, S. Zhou, C. Ohlsson and J. B. Richards, "Genomic atlas of the plasma metabolome prioritizes metabolites implicated in human diseases," *Nature Genetics,* vol. 55, no. 1, pp. 44-53, 1 2023.

[3] E. Rhee, J. Ho, M.-H. Chen, D. Shen, S. Cheng, M. Larson, A. Ghorbani, X. Shi, I. Helenius, C. O’Donnell, A. Souza, A. Deik, K. Pierce, K. Bullock, G. Walford, R. Vasan, J. Florez, C. Clish, J.-R. Yeh, T. Wang and R. Gerszten, "A Genome-wide Association Study of the Human Metabolome in a Community-Based Cohort," *Cell Metabolism,* vol. 18, no. 1, pp. 130-143, 7 2013.

[4] E. König, J. Rainer, V. V. Hernandes, G. Paglia, F. Del Greco M., D. Bottigliengo, X. Yin, L. S. Chan, A. Teumer, P. P. Pramstaller, A. E. Locke and C. Fuchsberger, "Whole Exome Sequencing Enhanced Imputation Identifies 85 Metabolite Associations in the Alpine CHRIS Cohort," *Metabolites,* vol. 12, no. 7, p. 604, 6 2022.

[5] G. Cadby, C. Giles, P. E. Melton, K. Huynh, N. A. Mellett, T. Duong, A. Nguyen, M. Cinel, A. Smith, G. Olshansky, T. Wang, M. Brozynska, M. Inouye, N. S. McCarthy, A. Ariff, J. Hung, J. Hui, J. Beilby, M.-P. Dubé, G. F. Watts, S. Shah, N. R. Wray, W. L. F. Lim, P. Chatterjee, I. Martins, S. M. Laws, T. Porter, M. Vacher, A. I. Bush, C. C. Rowe, V. L. Villemagne, D. Ames, C. L. Masters, K. Taddei, M. Arnold, G. Kastenmüller, K. Nho, A. J. Saykin, X. Han, R. Kaddurah-Daouk, R. N. Martins, J. Blangero, P. J. Meikle and E. K. Moses, "Comprehensive genetic analysis of the human lipidome identifies loci associated with lipid homeostasis with links to coronary artery disease," *Nature Communications,* vol. 13, no. 1, p. 3124, 6 2022.

[6] Nikpay M, Goel A, Won HH, Hall LM, Willenborg C, Kanoni S, Saleheen D, Kyriakou T, Nelson CP, Hopewell JC, Webb TR, Zeng L, Dehghan A and Alver M, "A comprehensive 1000 Genomes–based genome-wide association meta-analysis of coronary artery disease," *Nature Genetics,* vol. 47, no. 10, pp. 1121-1130, 10 2015.